



# Bis-neonicotinoid insecticides: Observed and predicted binding interactions with the nicotinic receptor

Ikuya Ohno<sup>a,b</sup>, Motohiro Tomizawaa<sup>c</sup>, Kathleen A. Durkin<sup>d</sup>, John E. Casida<sup>c</sup>, Shinzo Kagabu<sup>a,\*</sup>

<sup>a</sup> Department of Chemistry, Faculty of Education, Gifu University, Gifu 501-1193, Japan

<sup>b</sup> The United Graduate School of Agricultural Science, Gifu University, Gifu 501-1193, Japan

<sup>c</sup> Environmental Chemistry and Toxicology Laboratory, Department of Environmental Science, Policy and Management, University of California, Berkeley, CA 94720-3112, USA

<sup>d</sup> Molecular Graphics and Computational Facility, College of Chemistry, University of California, Berkeley, CA 94720-1460, USA

## ARTICLE INFO

### Article history:

Received 19 March 2009

Revised 22 April 2009

Accepted 6 May 2009

Available online 9 May 2009

### Keywords:

Acetylcholine binding protein

Bis-neonicotinoid insecticides

Imidacloprid

Nicotinic acetylcholine receptor

## ABSTRACT

The bis-pharmacophore approach applied to neonicotinoid insecticides reveals high binding affinity for heptamethylene bis-*N*<sup>3</sup>,*N*<sup>3'</sup>-imidacloprid fitting a nicotinic acetylcholine receptor model wherein the chloropyridine moieties contact loops E and F and the alkylene linker bridges these two distant domains.

© 2009 Elsevier Ltd. All rights reserved.

The nicotinic acetylcholine (ACh) receptor (nAChR) is the target for the neonicotinoids which account for one-fifth of the global insecticide market.<sup>1</sup> The principal compound is imidacloprid (IMI) (Fig. 1). ACh and other quaternary ammonium compounds play a unique role in the cholinergic nervous system.<sup>2</sup> Bisquaternary ammonium cholinergic ligands have many of the same effects with the interonium distance as a critical feature. In the neonicotinoids the chloropyridine or equivalent substituent takes the place of the ligand quaternary ammonium moiety. Bis-neonicotinoids with *N*<sup>3</sup>,*N*<sup>3'</sup>-alkylene-tethered linker moieties surprisingly have high insecticidal activities comparable to those of the parent monovalent compounds (Fig. 1).<sup>3,4</sup> The bis compounds act directly at the insect nAChR eliciting initial excitation and subsequent blockade<sup>3</sup> but in contrast they act as antagonists when co-applied with the agonist ACh<sup>5</sup> to the American cockroach abdominal ganglion.

The molecular recognition of bisquaternary ammonium compounds and curariform ligands has been predicted<sup>6,7</sup> using mollusk ACh binding protein (AChBP) as a structural surrogate of the extracellular ligand-binding domain of the nAChR.<sup>8</sup> Interestingly, the bisquaternary ammonium ligand conformations are recognized as having an extended geometry rather than being tightly-folded and the two ammonium heads contact two isolated subsites consisting of aromatic amino acid side chains in AChBP<sup>6</sup> and also in

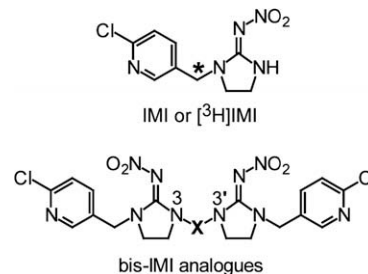


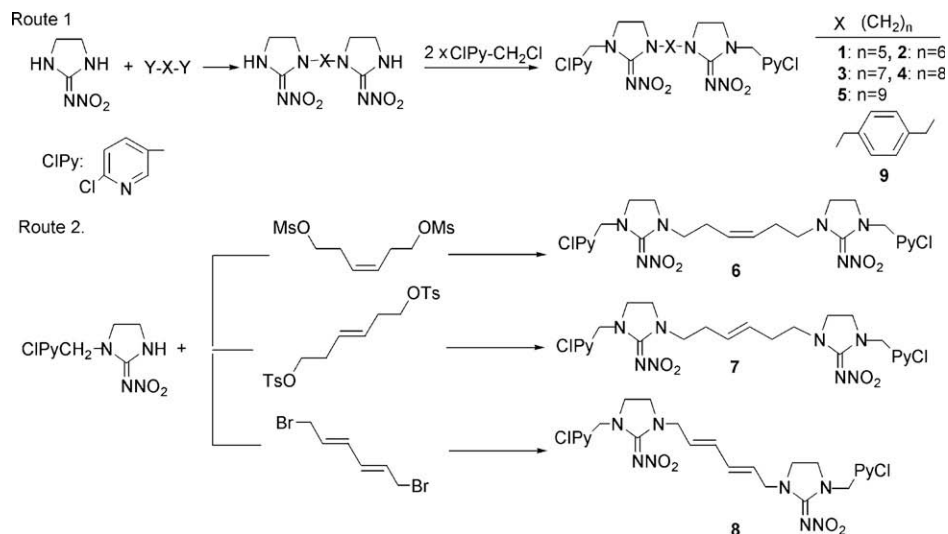
**Figure 1.** Neonicotinoid insecticide IMI and the bis analogues. Asterisk indicates position of tritium label.

ACh esterase.<sup>9</sup> In molecular recognition of monovalent neonicotinoids, resolved by chemical and structural biology approaches, the electronegative pharmacophore is nestled in a reversed direction compared with that of the ammonium functionality of the nicotinic agonist.<sup>10,11</sup> It is therefore fascinating to consider the structural uniqueness of divalent neonicotinoid molecular recognition.

This study examines the hypothesis that neonicotinoid insecticides with a bis pharmacophore retaining useful biological properties<sup>3,4</sup> might bind in a unique way at the nAChR. Bis-neonicotinoid compounds with various types of linkers (Fig. 1) are used here to understand the structure–activity relationships (SARs) in terms of binding affinity to the insect nAChR, thereby leading to in silico

\* Corresponding author. Tel.: +81 58 293 2253; fax: +81 58 293 2207.

E-mail address: kagabus@gifu-u.ac.jp (S. Kagabu).



**Scheme 1.** Preparation of bis-IMI analogues. Route 1 Y indicates Cl, Br, I, or OTs.

simulation of the binding location and conformation of the bis-neonicotinoid using the AChBP structural template.

Synthesis procedures for the bis-IMI analogues are summarized in Scheme 1. The preparation of compounds 1–5 and 9 was published previously.<sup>3,4</sup> The tethered molecules were prepared by the double introduction of the chloropyridinyl group to the pre-prepared tethered bis-nitroiminoimidazolidine (Route 1 in Scheme 1) or by the coupling of IMI with  $\alpha,\omega$ -functionalized linker (Route 2 in Scheme 1) as applied for the present new compounds (6–8).<sup>12</sup> The first route precludes any contamination by IMI itself, while the second route may result in the coexistence of IMI in the product mixture. Nevertheless, bis compounds can be cleanly separated from fast-eluted IMI on silica gel by using ethyl acetate as the eluent. The purity of the test compounds was finally confirmed on HPLC.

Binding affinities of bis-IMI analogues (Table 1) were evaluated with fruit fly (*Drosophila melanogaster*) brain nAChR.<sup>13</sup> Among the

compounds with C5–C9 alkylene-tethered linkers (1–5), C7 (3) showed optimal potency whereas others lost the affinity depending upon the number of methylene units (Fig. 2). The C2 and C10 analogues have greatly diminished potency at the housefly nAChR.<sup>3</sup> The SAR clearly indicates that the two IMI moieties linked with a suitable spacer length recognize independent subsites unique to each IMI counterpart in the ligand-binding domain. To understand the effects of alkylene-bridge conformations on fitting the binding pocket, three C6 analogues with *cis*, *trans*, and double *trans* configurations were examined. The *cis* compound (6) had similar effectiveness to that of the C6 alkylene parent (2) but the *trans* isomer (7) was 3.2- and 3.7-fold less potent than the *cis* isomer (6) and the C6 alkylene parent (2), respectively. The double *trans* compound (8) was 2.6-fold more potent than the single *trans* compound (7). The potency of compound 9 with an aromatic linker –CH<sub>2</sub>C<sub>6</sub>H<sub>4</sub>CH<sub>2</sub>– was 1.5-fold less active than the C6 *cis* isomer (6) but 2.1-fold more potent than the C6 *trans* isomer (7). These observations suggest that the optimal configuration of alkylene units, although relatively nonspecific, is determined by the regional binding domain involving various stabilization interactions.

Binding site interactions of bis compound 3 are simulated<sup>15</sup> with *Aplysia californica* AChBP based on its structure co-crystallized with bound IMI (protein data bank code 3C79)<sup>11</sup> (Fig. 3). The amino acids forming the binding pockets are structurally and functionally

**Table 1**  
Potencies of bis-IMI analogues as inhibitors of [<sup>3</sup>H]IMI binding to the *Drosophila* nAChR

No.	Linker moiety (X) <sup>a</sup>	K <sub>i</sub> ± SD <sup>b</sup> (μM)
1	–(CH <sub>2</sub> ) <sub>5</sub> –	5.35 ± 0.45
2	–(CH <sub>2</sub> ) <sub>6</sub> –	0.68 ± 0.027
3	–(CH <sub>2</sub> ) <sub>7</sub> –	0.14 ± 0.007
4	–(CH <sub>2</sub> ) <sub>8</sub> –	0.88 ± 0.121
5	–(CH <sub>2</sub> ) <sub>9</sub> –	1.38 ± 0.189
6		0.78 ± 0.10
7		2.49 ± 0.18
8		0.97 ± 0.081
9		1.18 ± 0.18

<sup>a</sup> Base structure of bis-IMI is given in Figure 1.

<sup>b</sup> K<sub>i</sub> = IC<sub>50</sub>/(1+[L]/K<sub>d</sub>) with [L] 4 nM and K<sub>d</sub> 5.6 nM.<sup>14</sup> All compounds had Hill coefficients of 0.92–1.07 indicating a single type of binding.

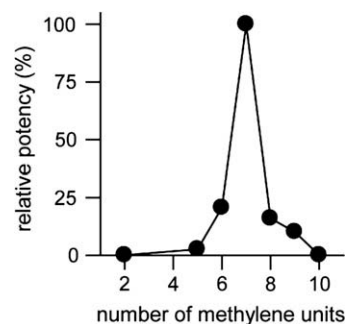


**Figure 2.** Relationship between length of alkylene-linker and relative binding potency of bis-IMI analogues. The relative potency (the optimal compound 3 with C7 linker defined as 100%) is taken from Table 1 and our previous report<sup>3</sup> giving the binding potencies of the C2 and C10 analogues to the housefly receptor (110 and 27 μM, respectively).

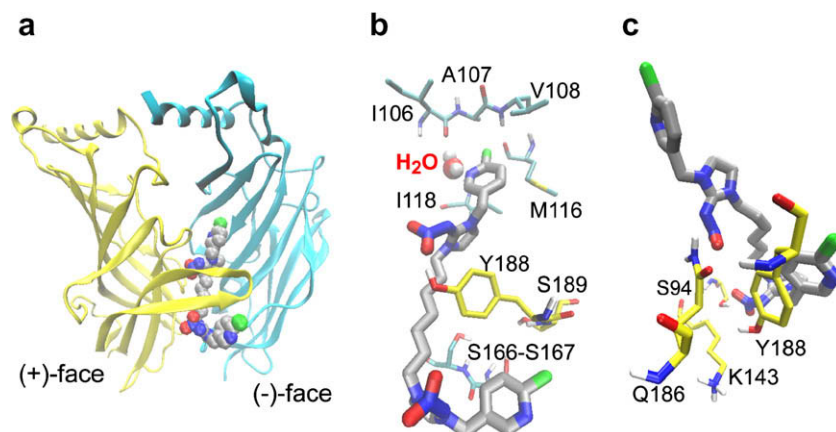


**Figure 3.** Simulated binding site interactions of bis-compound **3** with the *Aplysia* AChBP (protein data bank code 3C79)<sup>11</sup> structural surrogate of the extracellular domain of the nAChR. (a) Compound **3** is docked in the subunit interfacial binding pocket between the (+)-face (yellow) and (–)-face (aquamarine) subunits. One of five interfacial binding pockets is extracted and shown from the homopentameric AChBP structure. Snapshots for the molecular dynamic simulations emphasize interactions of the chloropyridine (b) and nitro (c) moieties with amino acids from the (+)-face (yellow) and (–)-face (aquamarine) subunits. The angle of view partially obscures the lower nitro moiety.

consistent not only in the diverse nAChRs but also in the AChBPs.<sup>10</sup> The A–E subunit interface of the AChBP–IMI complex is arbitrarily used for modeling since the homomeric AChBP pentamer has five identical binding pockets localized at subunit interfacial regions. The optimal bis compound **3** with the C7 alkylene linker, calculated to dock into the ligand-binding pocket with an energy of –9.42 kcal/mol, is nestled at the interface between the principal or (+)-face subunit and the complementary or (–)-face subunit (corresponding to  $\alpha$  and  $\beta$  or non- $\alpha$  subunits of nAChR, respectively). One of the two IMI counterparts (the upward one) binds to the same area where the single IMI molecule is accommodated with an especially nice overlay in the orientation of the chloropyridine moiety.<sup>10,11</sup> The other IMI portion of the bis compound faces toward the loop F niche on the complementary subunit. The C7 linker moiety is shown settled in the descending direction to bridge the two distant fields (loops E and F). Two chloropyridine moieties are presumably important for recognition of the bis neonicotinoid. One chloropyridine Cl van der Waals contacts the backbone of loop E (I106, A107, V108 and I118) (3–4 Å) and the pyridine N substantially interacts with the backbone O of I106 and NH of I118 (2–4 Å) via a water-bridge as observed in crystal and simulated structures of AChBPs liganded with pyridin-3-yl (or equivalent) nicotinic agonists.<sup>11,16</sup> The other chloropyridine Cl and N interact with loop F (2–5 Å). Our docking and molecular dynamics simulations show a range of conformations with similar energy wherein the pyridine N hydrogen-bonds the S166/S167 backbone and OH on loop F on the (–)-face subunit and the Cl contacts the backbone and side chains of Y188 and S189 on the (+)-face subunit. Consistent with this simulation, the bis-phenyl analogue replacing the bis-chloropyridine substituents has no biological activity (unpublished result). Therefore, definitely one and possibly both substituents play an important role in the binding interactions. The binding conformations seen in the molecular dynamics simulations show motions involving H-bonding interactions (forming and breaking) between each IMI moiety and its binding niche. Especially, the downward IMI pyridinyl N interacts with the S166 or S167 OH and the nitro O contacts side chains S94, K143, Q186, and Y188 on the (+)-face subunit. Other interactions in this area may be mediated via water(s) as these residues are near the protein surface. Accordingly, the loop F niche may embrace, in a different way, alternative pharmacophore positioning of bis analogues depending on the length of linker.

In summary, the insecticidal bis-neonicotinoid compounds bind in a unique mode at the nAChR depending upon the linker size.

Two chloropyridine moieties contact loops E and F and the linker bridges these two disparate and distant subsites. The present SAR findings reveal an intriguing molecular recognition mode at the nAChR structural model, thereby prompting photoaffinity labeling or X-ray crystallographic approach to facilitate receptor structure-guided design of novel insecticidal compounds.

#### Acknowledgments

M.T. and J.E.C. were funded by National Institute of Environmental Health Science Grant R01 ES08424. J.E.C. was supported by the William Muriece Hoskins Chair in Chemical and Molecular Entomology. K.A.D. was supported by National Science Foundation Grant CHE-0233882.

#### References and notes

- Tomizawa, M.; Casida, J. E. *Annu. Rev. Pharmacol. Toxicol.* **2005**, *45*, 247.
- Paton, W. D. M.; Zaimis, E. J. *Pharmacol. Rev.* **1952**, *411*, 269.
- Kagabu, S.; Iwaya, K.; Konishi, H.; Sakai, A.; Itazu, Y.; Kiriya, K.; Nishimura, K. *J. Pestic. Sci.* **2002**, *27*, 249.
- (a) Kagabu, S.; Itazu, Y.; Nishimura, K. *J. Pestic. Sci.* **2004**, *29*, 40; (b) Kagabu, S.; Itazu, Y.; Nishimura, K. *J. Pestic. Sci.* **2006**, *31*, 146; (c) Kagabu, S. *Jpn. Kokai Tokkyo Koho*, JP 2008291021 A, 2008.
- Ihara, M.; Hirata, K.; Ishida, C.; Kagabu, S.; Matsuda, K. *Neurosci. Lett.* **2007**, *425*, 137.
- Carter, C. R. J.; Cao, L.; Kawai, H.; Smith, P. A.; Dryden, W. F.; Raftery, M. A.; Dunn, S. M. *J. Biochem. Pharmacol.* **2007**, *73*, 145.
- Gao, F.; Bren, N.; Little, A.; Wang, H.-L.; Hansen, S. B.; Talley, T. T.; Taylor, P.; Sine, S. M. *J. Biol. Chem.* **2003**, *278*, 23020.
- (a) Brejck, K.; van Dijk, W. J.; Klaassen, R. V.; Schuurmans, M.; van der Oost, J.; Smit, A. B.; Sixma, T. K. *Nature* **2001**, *411*, 269; (b) Hansen, S. B.; Sulzenbacher, G.; Huxford, T.; Marchot, P.; Taylor, P.; Bourne, Y. *EMBO J.* **2005**, *24*, 3635; (c) Tomizawa, M.; Maltby, D.; Medzihradsky, K. F.; Zhang, N.; Durkin, K. A.; Presley, J.; Talley, T. T.; Taylor, P.; Burlingame, A. L.; Casida, J. E. *Biochemistry* **2007**, *46*, 8798.
- Harel, M.; Schalk, I.; Ehret-Sabatier, L.; Bouet, F.; Goeldner, M.; Hirth, C.; Axelsen, P. H.; Silman, I.; Sussman, J. L. *Proc. Natl. Acad. Sci. U.S.A.* **1993**, *90*, 9031.
- (a) Tomizawa, M.; Talley, T. T.; Maltby, D.; Durkin, K. A.; Medzihradsky, K. F.; Burlingame, A. L.; Taylor, P.; Casida, J. E. *Proc. Natl. Acad. Sci. U.S.A.* **2007**, *104*, 9075; (b) Tomizawa, M.; Maltby, D.; Talley, T. T.; Durkin, K. A.; Medzihradsky, K. F.; Burlingame, A. L.; Taylor, P.; Casida, J. E. *Proc. Natl. Acad. Sci. U.S.A.* **2008**, *105*, 1728; (c) Tomizawa, M.; Casida, J. E. *Acc. Chem. Res.* **2009**, *42*, 260.
- Talley, T. T.; Harel, M.; Hibbs, R. H.; Radić, Z.; Tomizawa, M.; Casida, J. E.; Taylor, P. *Proc. Natl. Acad. Sci. U.S.A.* **2008**, *105*, 7606.
- (a) All melting points (mp) are uncorrected. IR spectra were measured with a Perkin Elmer FTIR 1600 spectrometer. <sup>1</sup>H and <sup>13</sup>C NMR spectra were recorded using a JEOL ECA-500 spectrometer at 500 and 125 MHz, respectively. The chemical shifts were recorded in  $\delta$  (ppm) and the coupling constants  $J_{H-H}$  in hertz. Mass spectra were recorded at 70 eV with the JEOL JMS-700 instrument. For biological assays the purities of the compounds were confirmed by HPLC (Pump; Bip-1, JASCO, UVDEC 100 VI, JASCO; 270 nm) with a 5-mm Lichrosorb

RP-18 column (Merck) using acetonitrile/water 1:1. 1,6-Bis-[(2-chloro-5-pyridinylmethyl)-2-nitriminoimidazolidin-3-yl]-3(Z)-hexene (**6**). Sodium hydride (60% oil dispersion, 80 mg, 2 mmol) was added portionwise to a stirred solution of IMI (514 mg, 2 mmol) in dimethylformamide (DMF) (30 ml) with ice cooling. After the addition, the stirring was continued for a further 30 min at room temperature. The reaction mixture was cooled again with an ice bath and treated with 3(Z)-hexene 1,6-bismesilate (Eya et al., 1990, see **b** below) (186 mg, 0.75 mmol). The mixture was stirred overnight at room temperature and then 9 h at 50 °C. After quenching the reaction with a drop of acetic acid, the DMF was distilled off. The residual semi-solid was rinsed sequentially with water and ether. The remaining solid was subjected to column chromatography on silica gel with ethyl acetate until no further IMI was detected in the fractions, then the elution was continued by replacing the eluting medium with ethyl acetate/methanol 5:1. The separated product was recrystallized from ethanol. The separated product was recrystallized from ether/methanol 1:1. Yield: 23 mg (5%), mp 93–95 °C. <sup>1</sup>H NMR (CDCl<sub>3</sub>): 2.43 (2 × 2H, m), 3.32 (2 × 2H, m), 3.64 (2 × 2H, m), 3.84 (2 × 2H, m), 4.48 (2 × 2H, s), 5.48 (2 × 1H, m), 7.36 (2 × 1H, d, *J* = 8.3 Hz), 7.70 (2 × 1H, dd, *J* = 8.3 Hz, *J* = 2.3 Hz), 8.33 (2 × 1H, d, *J* = 2.3 Hz). <sup>13</sup>C NMR (CDCl<sub>3</sub>): 25.2, 45.3, 46.4, 46.7, 47.4, 124.9, 128.1, 129.2, 139.2, 149.5, 151.8, 161.1. FAB-HRMS for C<sub>24</sub>H<sub>28</sub>Cl<sub>2</sub>N<sub>10</sub>O<sub>4</sub>: Calcd. (+H<sup>+</sup>), 591.1750; Found, 591.1767. 1,6-Bis-[(2-chloro-5-pyridinylmethyl)-2-nitriminoimidazolidin-3-yl]-3(E)-hexene (**7**). This product was obtained similarly using 3(E)-hexene 1,6-bistosylate in place of 3(Z)-hexene 1,6-bismesilate. Yield: 132 mg (30%), mp 129–130 °C. <sup>1</sup>H NMR (CDCl<sub>3</sub>): 2.33 (2 × 2H, m), 3.36 (2 × 2H, t, *J* = 6.8 Hz), 3.63 (2 × 2H, m), 3.76 (2 × 2H, m), 4.77 (2 × 2H, s), 5.48 (2 × 1H, m), 7.34 (2 × 1H, d, *J* = 8.1 Hz), 7.71 (2 × 1H, dd, *J* = 8.1 Hz, *J* = 2.6 Hz), 8.33 (2 × 1H, d, *J* = 2.6 Hz). <sup>13</sup>C NMR (CDCl<sub>3</sub>): 29.9, 45.2, 45.7, 46.2, 47.4, 124.9, 128.9, 129.2, 139.3, 149.6, 151.8, 161.4. FAB-HRMS for C<sub>24</sub>H<sub>28</sub>Cl<sub>2</sub>N<sub>10</sub>O<sub>4</sub>: Calcd. (+H<sup>+</sup>), 591.1750; Found, 591.1772. 1,6-Bis-[(2-chloro-5-pyridinylmethyl)-2-nitriminoimidazolidin-3-yl]-2(E),4(E)-hexadiene (**8**). This reaction was carried out similarly to that for compound **7** using 2(E),4(E)-1,6-dibromohexadiene (Spangler et al., 1989, see **c** below) in place of 3(E)-hexene 1,6-bistosylate. The work-up was as follows. After evaporating the DMF, the remaining solid was washed successively with water and methanol, and collected on a filter paper with suction. The crude crops were repeatedly recrystallized from hot methanol. Yield 268 mg (61%), mp 215–217 °C. <sup>1</sup>H NMR δ (DMSO-*d*<sub>6</sub>): 3.64 (2 × 4H, overlap, m), 3.84 (2 × 2H, m), 4.42 (2 × 2H, s), 5.67 (2 × 1H, m), 6.24 (2 × 1H, m), 7.51 (2 × 1H, d, *J* = 8.3 Hz), 7.75 (2 × 1H, dd, *J* = 8.5 Hz, *J* = 2.9 Hz), 8.32 (2 × 1H, d, *J* = 2.9 Hz). <sup>13</sup>C NMR δ (DMSO-*d*<sub>6</sub>): 45.8, 46.0, 46.8, 48.2, 124.8, 127.4, 131.1, 133.3, 140.0, 149.9, 150.2, 160.9. FAB-

HRMS for C<sub>24</sub>H<sub>26</sub>Cl<sub>2</sub>N<sub>10</sub>O<sub>4</sub>: Calcd (+H<sup>+</sup>), 589.1594. Found, 589.1591. (b) Eya, B. K.; Otsuka, T.; Kubo, I.; Wood, D. L. *Tetrahedron* **1990**, *46*, 2695. (c) Spangler, C. W.; McCoy, R. K.; Dembek, A.A.; Sapochak, L. S.; Gates, B. D. *J. Chem. Soc. Perkin Trans. 1*, **1989**, 151.

13. Tomizawa, M.; Latli, B.; Casida, J. E. *J. Neurochem.* **1996**, *67*, 1669.
14. Zhang, N.; Tomizawa, M.; Casida, J. E. *Neurosci. Lett.* **2004**, *371*, 56.
15. (a) Structures were docked to the (+) and (–) interface of the AChBP crystal structure (chains A and E from 3C79) using the GLIDE algorithm in MAESTRO (GLIDE 5.0, MAESTRO 8.5, Schrödinger, LLC, New York, NY, 2008) (Friesner et al., 2004, see **b** below). Receptors were prepared for docking by addition of hydrogen atoms and the removal of the co-crystallized ligands and other nonprotein moieties. The Glide receptor grid was cubic, 40 Å per side, and centered on the region occupied by the ligand in the original protein structure. The docking algorithm does a spatial fit of the ligand to the receptor grid, followed by minimization and scoring of hits based on a discretized ChemScore function (Eldridge et al., 1997, see **c** below; Baxter et al., 1998, see **d** below). The ligand was flexibly docked using standard precision and the top hits were examined. 3C79 was additionally iteratively minimized and subjected to a side chain conformational search with a docked ligand because the binding pocket of this structure originally contained only the monomer IMI and needed to flex to accommodate larger ligands in an energetically favorable manner. (b) Friesner, R. A.; Banks, J. L.; Murphy, R. B.; Halgren, T. A.; Klicic, J. J.; Mainz, D. T.; Repasky, M. P.; Knoll, E. H.; Shelley, M.; Perry, J.K.; Shaw, D.E.; Francis, P.; Shenkin, P. S. *J. Med. Chem.* **2004**, *47*, 1739. (c) Eldridge, M. D.; Murray, C. W.; Auton, T. R.; Paolini, G. V.; Mee, R. P. *J. Comput. Aided Mol. Des.*, **1997**, *11*, 425. (d) Baxter, C. A.; Murray, C. W.; Clark, D. E.; Westhead, D. R.; Eldridge, M. D. *Proteins*, **1998**, *33*, 367. (e) Molecular dynamics simulations were performed on low energy docking hits using Desmond 2.0 (Bowers et al., 2007, see **f** below). The simulations included the ligand, receptor (chains A and E of 3C79) and a cubic box of water (84–90 Å per side depending of the receptor orientation) fully enclosing the complex surrounded by periodic boundary conditions. Simulations were run at 300 K for between 1 and 10 ns using a 2 fs timestep with the SHAKE algorithm and a Berendsen thermostat with 1 ps of heating. (f) Bowers, K.J.; Dror, R. O.; Shaw, D. E. *J. Comput. Phys.* **2007**, *221*, 303.
16. (a) Celie, P. H. N.; van Rossum-Fikkert, S. E.; van Dijk, W. J.; Brejc, K.; Smit, A. B.; Sixma, T. K. *Neuron* **2004**, *41*, 907; (b) Ihara, M.; Okajima, T.; Yamashita, A.; Oda, T.; Hirata, K.; Nishiwaki, H.; Morimoto, T.; Akamatsu, M.; Ashikawa, Y.; Kuroda, S.; Mega, R.; Kuramitsu, S.; Sattelle, D. B.; Matsuda, K. *Invert. Neurosci.* **2008**, *8*, 71; (c) Ohno, I.; Tomizawa, M.; Durkin, K. A.; Casida, J. E.; Kagabu, S. *J. Agric. Food Chem.* **2009**, *57*, 2436.